Tetrahedron 68 (2012) 1590–1594

Contents lists available at SciVerse ScienceDirect

Tetrahedron

journal homepage: www.elsevier.com/locate/tet

Tetrathiafulvalene-annulated dipyrrolylquinoxaline: the effect of fluoride on its optical and electrochemical behaviors

Hong-Peng Jia [a], John C. Forgie [b], Shi-Xia Liu [a,*], Lionel Sanguinet [c], Eric Levillain [c], Franck Le Derf [c,d], Marc Sallé [c], Antonia Neels [e], Peter J. Skabara [b], Silvio Decurtins [a]

[a] Departement für Chemie und Biochemie, Universität Bern, Freiestrasse 3, CH-3012 Bern, Switzerland
[b] WestCHEM, Department of Pure and Applied Chemistry, University of Strathclyde 295, Cathedral Street, Glasgow G1 1XL, UK
[c] Université d'Angers, MOLTECH-Anjou, CNRS UMR 6200, 2 Bd Lavoisier, 49045 Angers Cedex, France
[d] Université de Rouen, UMR CNRS COBRA 6014, 55 rue Saint Germain, 27000 Evreux, France
[e] XRD Application LAB, CSEM Centre Suisse d'Electronique et de Microtechnique SA, Jaquet-Droz 1, Case postale, CH-2002 Neuchâtel, Switzerland

ARTICLE INFO

Article history:
Received 15 September 2011
Received in revised form 24 November 2011
Accepted 28 November 2011
Available online 6 December 2011

Keywords:
Tetrathiafulvalene
Electrooptical sensor
Anions
Electrochemical polymerization
Charge transfer

ABSTRACT

A tetrathiafulvalene donor has been annulated to 2,3-di(1*H*-2-pyrrolyl)quinoxaline affording a new chemosensor **1**, which shows a unique optical selectivity and reactivity for the fluoride ion over other anions in CH_2Cl_2 leading to a colorimetric response. Electrochemical polymerization of **1** occurred in the presence of fluoride.

1. Introduction

The development of highly sensitive anion sensors has attracted considerable attention due to the fact that a large number of biological processes involve molecular recognition of anionic species.[1] In recent decades, a wide variety of naked-eye colorimetric sensors have been reported.[1,2] However, only a few are able to differentiate selectively between anionic substrates of similar basicity and surface charge density.[2] Thus, selective and reliable sensing of anions is a quite challenging area of research. To increase the overall reliability of the sensing process, a rational strategy involves attainment of two independent modes of signal transduction in the sensor material. Although known, such materials are still rare.[3] Among the many inorganic anions, fluoride is of particular interest because of its beneficial (e.g., prevention of dental caries and treatment of osteoporosis) as well as detrimental (e.g., fluorosis) roles.[4] As a consequence, 2,3-di(1*H*-2-pyrrolyl)quinoxaline (DPQ)-based fluoride sensors have been elaborately developed.[1,3d–f,5] Quite surprisingly, only three examples concerned the use of the DPQ building block for the preparation of sensors, which generate strong colorimetric and electrochemical signals.[3d–f] In all cases, a common rationale has been applied, namely, they all contain electron-withdrawing moieties (a conductive polymer, quinone or Co(III) complex), which render the pyrrole NH protons more acidic, thereby leading to enhanced receptor–substrate affinity.

In an effort to explore a DPQ system with dual modes of signal transduction, herein we introduce the new tetrathiafulvalene (TTF)-fused DPQ derivative **1** (Scheme 1). TTF and its derivatives, as strong π-donors, are important components in the field of organic conductors and superconductors.[6] It is noteworthy that they are not yet fully explored as anion chemosensors[7] in spite of an extensive investigation on their application in the field of molecular switches and sensors.[6b,c] Quite recently, the Sessler group reported a dual optical-electrochemical chemosensor for dihydrogen phosphate by incorporation of TTF into diindolylquinoxaline.[8] In the present

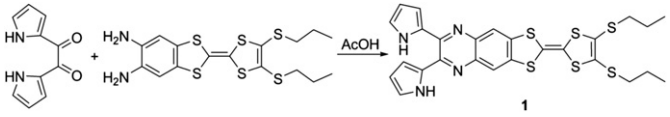

Scheme 1. Synthesis of sensor **1**.

* Corresponding author. Tel.: +41 31 631 4296; fax: +41 31 631 4399; e-mail address: liu@iac.unibe.ch (S.-X. Liu).

0040-4020/$ – see front matter © 2011 Elsevier Ltd. All rights reserved.
doi:10.1016/j.tet.2011.11.087

contribution, we present the synthesis, structure and fluoride anion recognition properties of compound **1**.

2. Results and discussion

The synthesis of the target sensor **1** is accomplished in 50% yield by condensation of 5,6-diamino-2-(4,5-bis(propylthio)-1,3-dithio-2-ylidene)benzo[*d*][1,3]dithiole[9] with 1,2-di(1*H*-2-pyrrolyl)-ethane-1,2-dione[10] in glacial acetic acid. It was unambiguously characterized by spectroscopic analyses and also by single crystal X-ray analysis.

The sensor **1** crystallizes as solvate-free orange rods in a centrosymmetric orthorhombic space group (*Pbca*). Fig. 1 shows the asymmetric unit comprising the complete molecule with one disordered propyl substituent (C17, C17A, C18, and C18A are half occupied). In contrast to the related DPQ derivatives,[5c–e] **1** adopts a conformation where one pyrrolic NH proton points toward a nitrogen atom of the pyrazine ring and the other one turns away. Due to the close proximity of the two pyrrole rings, they are twisted out of the parent skeleton. The torsional angles of the two pyrrole rings with respect to the least-squares plane consisting of the TTF core and quinoxaline unit with an rms deviation of only 0.04 Å, are 55.9(1)° and 18.6(2)°. A least-squares plane through the atoms of the TTF core alone reveals an rms deviation of only 0.02 Å. The bond lengths in the DPQ and TTF moieties are in the expected range in comparison with literature values.[5c–e,11]

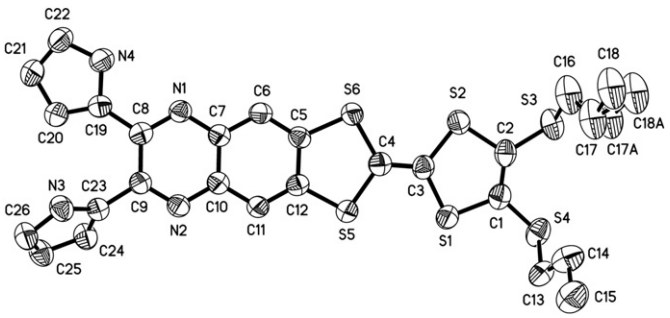

Fig. 1. X-ray crystal structure of **1** (ORTEP, thermal ellipsoids set at the 50% probability level). Hydrogen atoms are omitted for clarity.

In the crystal lattices (Fig. S1), the molecules are stacked along the *a*-axis through intermolecular (pyrrole)NH···N (pyrazine) hydrogen bonds, leading to a parallel head-to-head alignment with intermolecular S···S contacts of 3.7 Å and 3.9 Å.

The anion binding affinity of **1** was evaluated by monitoring its UV–vis spectra. The titration experiments were performed in a CH_2Cl_2/CH_3CN mixture using fluoride, chloride, bromide, cyanide, perchlorate, acetate, benzoate, and dihydrogen phosphate anions as tetra-*n*-butylammonium salts. Surprisingly, whereas diindolylquinoxaline analogues show a good selectivity for binding the dihydrogen phosphate anion,[8,12] no evidence of such affinity binding could be detected with compound **1**, which presents instead a strong selectivity for the fluoride anion. Fig. 2 presents the changes in the UV–vis spectra of **1** as a function of [F^-]. A quite intricate behavior is observed. As expected, compound **1** shows strong broad absorption bands at approximately 480 nm and 320 nm. The former can be readily attributed to a spin-allowed π–π* intraligand charge-transfer transition (^{1}ILCT) with the TTF subunit as an electron donor and the DPQ subunit as an acceptor while the latter corresponds to π–π* transitions of the TTF unit. Upon the addition of increasing quantities of fluoride, the broad absorption band at 480 nm gradually disappears and a new absorption band at 510 nm concomitantly emerges, with a significant

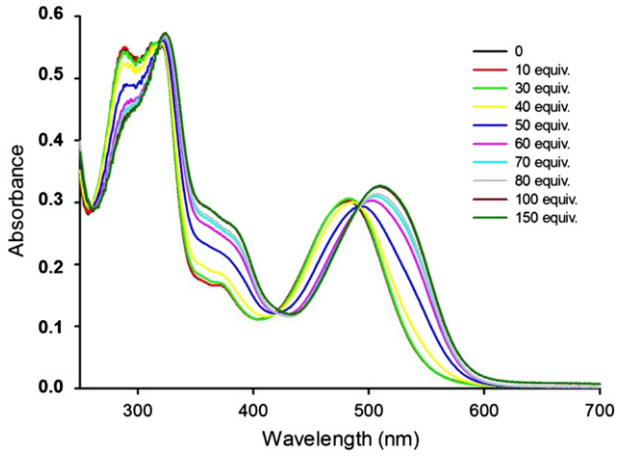

Fig. 2. UV–vis spectral changes of sensor **1** (10^{-5} M in CH_2Cl_2/CH_3CN (1:1)) upon the addition of TBAF.

color change from brown to pink that can be observed by the naked eye. This change may be attributed to a deprotonation-induced process, as previously observed during the titration of diindolylquinoxaline analogues with the basic fluoride anion.[13] A remarkable feature is the occurrence of a quite well defined isosbestic point at 490 nm indicating that **1** coexists with only one species upon addition of TBAF. The affinity constant of K_a=640 M^{-1} in CH_2Cl_2/CH_3CN for sensor **1** and F^- was obtained from titration profiles at 380 nm and 510 nm (Fig. S2) by the Benesi–Hildebrand method.

Interestingly, the presence of other tested anions does not cause any detectable changes in the UV–vis spectra, even when more than 100 stoichiometric ratios of anions are added (Fig. S3).

To get deeper insights into the interactions between **1** and fluoride, ^{1}H NMR titration experiments were performed in CD_2Cl_2/CD_3CN (1:1) (Fig. 3). For low fluoride concentrations (0–3 equiv), the NH proton resonance at 9.95 ppm becomes sharp and shifts significantly upfield. Also, the other aromatic proton resonances of **1** exhibit a small upfield shift. These results tend to indicate the formation of N–H···F^- hydrogen bonding under these conditions. With a further course of addition (from 5 equiv of F^- on), the NH proton signal completely disappears (Fig. S4), suggesting that the deprotonation of **1** now takes place in accordance with

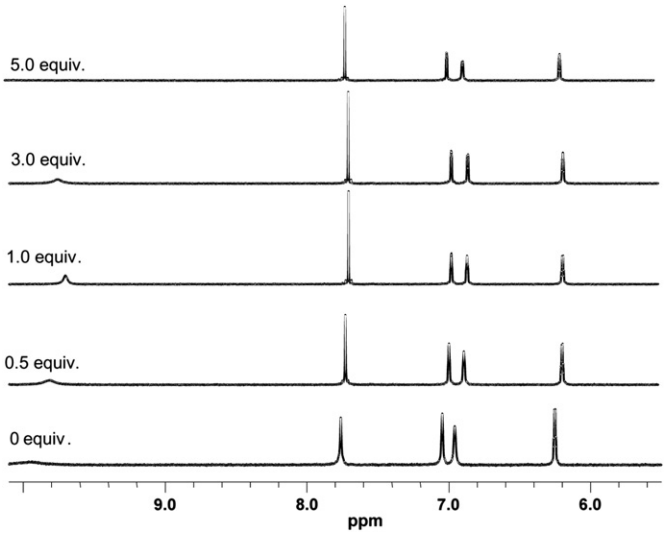

Fig. 3. ^{1}H NMR spectra of compound **1** (1.45×10^{-2} M in CD_2Cl_2/CD_3CN (1:1)) upon the addition of successive aliquots of TBAF (CD_2Cl_2).

aforementioned observations made from UV–vis spectroscopic titration. It can be deduced therefore that the presence of F^- not only induces a formation of a H-bonding species but leads also to a deprotonation process.

As discussed above, sensor **1** is expected to show a built-in optical-electrochemical dual-signaling for anions. Specifically, interactions between the DPQ unit and the tested anions lead to a variation in the π-electron donating ability of the TTF moiety. As a test of this hypothesis, cyclic voltammetry (CV) titrations have been performed in a CH_2Cl_2/CH_3CN (9:1) mixture. Surprisingly, addition of any tested anions led to a dramatic variation in both, reversibility and intensity of the two redox waves (Fig. S5), indicative of electron-transfer reactions, most probably coupled with a complex sequence of chemical follow-up processes. Although a detailed study hereof would be outside the scope of this work, we have further investigated the specific effect of F^- on the redox behavior of compound **1**. As illustrated in Fig. 4, in the absence of F^-, **1** displays two reversible one-electron oxidation waves at 0.19 V and 0.48 V (vs Fc/Fc^+), corresponding to the successive generation of the $TTF^{\bullet+}$ radical cation and the TTF^{2+} dication. Upon the addition of F^-, an initial anodic shift followed by a significant increase in the current of both oxidation processes is observed, presumably due to the formation of N–H···F^- hydrogen bonding pulling electron density away from the TTF moiety, together with the polymer growth in the vicinity of the working electrode. The latter was observed by the formation of a red film on the working electrode. Taking into account UV–vis spectroscopic titrations, we can assume that **1** shows a unique optical selectivity and reactivity for the fluoride ion over other anions with dual modes of signal transduction.

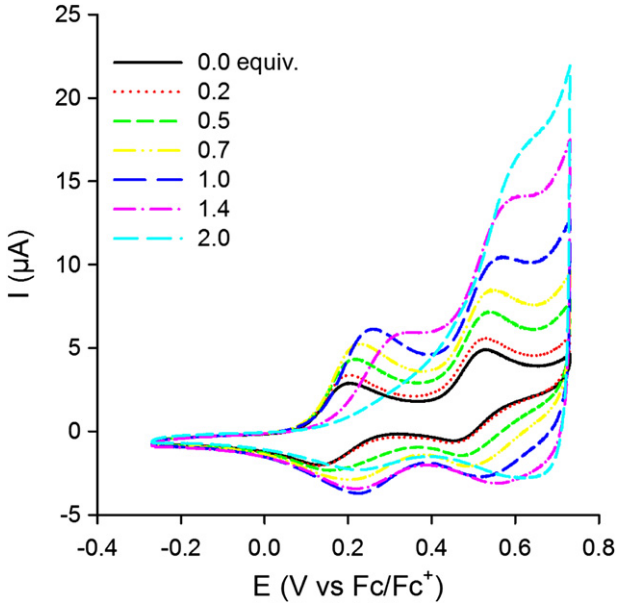

Fig. 4. CV behavior of sensor **1** upon the addition of successive aliquots of TBAF; [**1**]= 2.24×10^{-4} M in CH_2Cl_2/CH_3CN (9:1), $TBAPF_6$ (0.1 M), 293 K, 200 mV/s.

In order to arrive at a better understanding of the polymer formation during the period of CV titrations, a detailed study of electropolymerization of **1** has been carried out. Monomer **1** can be readily polymerized electrochemically by repetitive cycling over its anodic redox-active range. The growing of the polymer film is illustrated by Fig. 5, exhibiting the electrochemical response under potentiodynamic conditions. As the monomer is oxidized, significant spin density must reside over the pyrrole units for polymerization to take place. The polymer was grown onto a glassy carbon

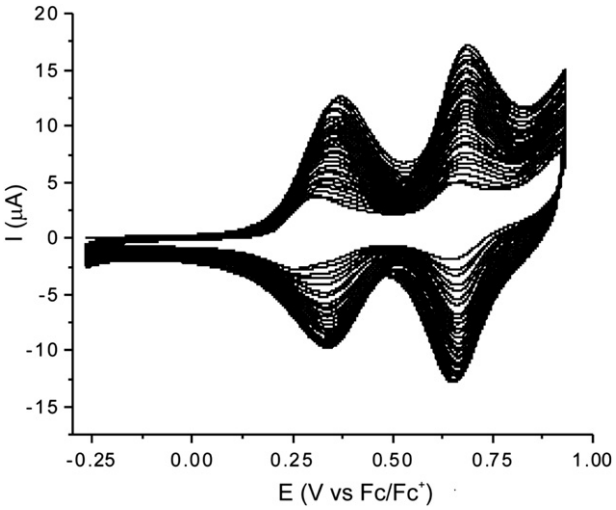

Fig. 5. Growth of polymer by cyclic voltammetry in CH_2Cl_2, using a glassy carbon working electrode, Ag wire pseudo-reference electrode, platinum wire counter-electrode, $TBAPF_6$ as the supporting electrolyte (0.1 M), [**1**]=2×10^{-4} M, scan rate 100 mV/s. The data are referenced to the Fc/Fc^+ redox couple.

electrode first so it could be subsequently characterized in monomer-free solution by CV. Both monomer and polymer exhibit two reversible oxidation and two irreversible reduction waves (Figs. 6 and 7), corresponding to the oxidation of TTF and the reduction of DPQ units, respectively. The half-wave potentials for the oxidation of the polymer are $E^1_{1/2}$=+0.40 V and $E^2_{1/2}$=+0.74 V. Irreversible reduction peaks are observed at −0.71 V and −1.85 V for the polymer. The reduction processes for the monomer and polymer are attributed to the reduction of the nitrogen-containing units. In the case of the polymer, these units are part of the main chain and thus have lower potentials as a result of the extended conjugation. The corresponding electrochemical HOMO–LUMO gaps of 1.90 eV and 1.54 eV for **1** and its polymer can be deduced

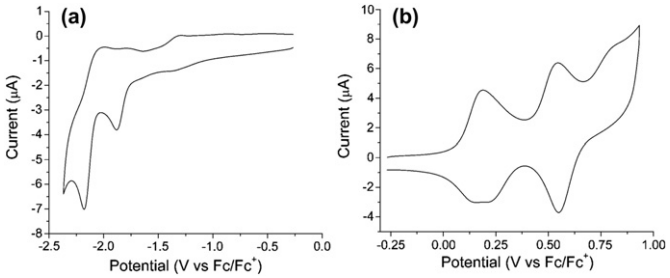

Fig. 6. Cyclic voltammograms of monomer **1** in CH_2Cl_2 showing (a) reduction and (b) oxidation processes (conditions as for Fig. 5).

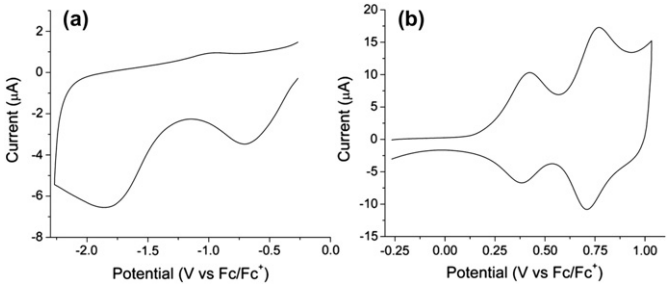

Fig. 7. Cyclic voltammograms of polymer of **1** as a film, showing (a) reduction and (b) oxidation processes (conditions as for Fig. 5).

from the difference between the onsets of reduction and oxidation processes as shown in Table 1. The data for all redox processes are referenced to ferrocene and the specific HOMO and LUMO levels of the monomer and polymer were calculated by subtracting the

Table 1
Onset oxidation and reduction potentials (V vs Fc/Fc^+), HOMO and LUMO levels (eV), and electrochemical band gaps E_g (eV) of monomer **1** and its polymer

Compound	E^{ox1}_{onset}	HOMO	E^{red1}_{onset}	LUMO	E_g
1	0.17	−4.97	−1.73	−3.07	1.9
Polymer	0.24	−5.04	−1.30	−3.50	1.54

onset of the first oxidation and reduction peaks from the known HOMO of ferrocene (−4.8 eV). Furthermore, the optical HOMO–LUMO gaps for the monomer and polymer are estimated from the onset of the lowest energy electronic absorptions in the corresponding UV–vis spectra (Fig. 2 in solution and Fig. 8 in the film) to be 2.2 eV and 1.9 eV, respectively. The discrepancy between the electrochemically and optically determined HOMO–LUMO gaps, particularly for the polymer, arises from the fact that the TTF unit is the dominant redox centre for the first oxidation process and therefore the true HOMO is separate from the longest wavelength absorption transition, which is expected to be a $\pi-\pi^*$ process involving other components of the molecule.

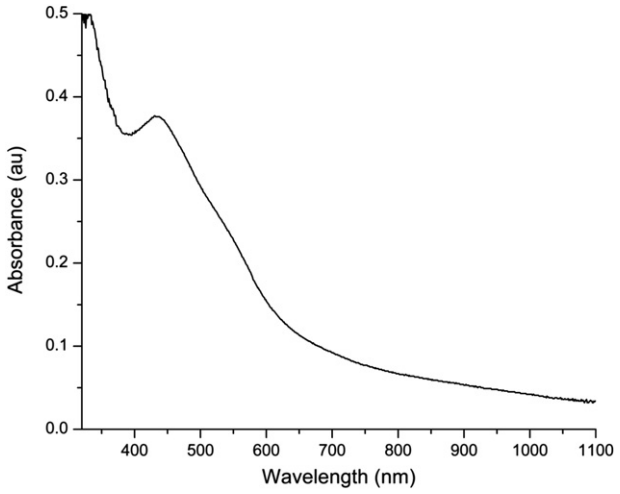

Fig. 8. Absorption spectrum of polymer of **1** as a thin film deposited on ITO glass.

The absorption spectrum of the polymer was recorded by growing the polymer onto an ITO coated glass slide using repetitive cycling as above but with a greater number of cycles. The resultant red polymer showed a peak at 436 nm and allowed a comparison with the red films produced by the addition of fluoride ion during cycling to confirm the occurrence of electropolymerisation. The absorption spectrum of a freshly made film clearly shows an intense absorption band at 436 nm, attributed to the $\pi-\pi^*$ transitions of the resulting polymer (Fig. 8). On the other hand, polymer growth was observed over six cycles in the presence of 2 equiv of F^- giving rise to the identical UV–vis spectrum. Further repetitive scanning leads to the disappearance of two redox waves, which is consistent with the aforementioned observation by CV experiments. It can be deduced therefore that the resultant polymer forms an insulating barrier that does not allow current response to be recorded. As the film is oxidized over repeated scans, it is possible that the resulting carbocations undergo nucleophilic attack by the fluoride anions present in solution. This would result in saturated sites along the polymer backbone and would explain the observation of an insulating effect.

3. Conclusion

In conclusion, the receptor **1** with a built-in optical-electrochemical dual-signaling functionality is reported. The highly selective sensing of fluoride is visible by the naked eye, observed by a color change of the substrate in solution. Interestingly, electrochemical polymerization of **1** unambiguously occurred in the presence of fluoride. Efforts toward the development of sensors for other biologically important anions as well as the attainment of materials capable of anion sensing in the presence of water are under way.

4. Experimental section

4.1. Equipment

^1H and ^{13}C NMR spectra were acquired on a Bruker AC 300 spectrometer operating at 300.18 MHz and 75.5 MHz, respectively: chemical shifts are reported in parts per million referenced to residual solvent protons. The following abbreviations were used s (singlet), d (doublet), t (triplet) and m (multiplet). FTIR data was collected on a Perkin–Elmer Spectrum One spectrometer. Mass spectrum was obtained on an AutoSpecQ spectrometer for the EI ionization mode (70 eV). Elemental analysis was performed on a Carlo Erba EA 1110 CHN apparatus.

4.2. UV–vis titration experiments

UV–vis spectra of **1** were performed in CH_2Cl_2/CH_3CN (1:1) on Bruker Lambda 2 spectrometer at room temperature in the presence of increasing amounts of the TBA salt of the anions of study. The concentration of the receptor **1** was 10^{-5} mol L^{-1}.

4.3. ^1H NMR titration experiments

NMR spectra were recorded at 500.13 MHz and all measurements were carried out at 298 K. A solution of the receptor **1** (1.45×10^{-2} M in CD_2Cl_2/CD_3CN (1:1)) was prepared and stepwise additions of a solution of hydrated tetrabutylammonium fluoride were performed until no additional changes in chemical shifts were observed.

4.4. Electrochemistry

Dichloromethane and acetonitrile (HPLC grade, Acros) were used as received. Tetra-*n*-butylammonium hexafluorophosphate ($TBAPF_6$, electrochemical grade, Fluka) is recrystallized from ethanol prior to use.

Cyclic voltammetry (CV) was performed in a three-electrode cell equipped with a platinum millielectrode, a platinum wire counter-electrode, and a silver wire used as a quasi-reference electrode. The voltammograms were recorded on a potentiostat/galvanostat (BioLogic—SP2) driven by the EC-Lab V 9.98 software. All electrochemical experiments were carried out under a dry and oxygen-free atmosphere ($H_2O<1$ ppm, $O_2<1$ ppm) in a mixture of CH_2Cl_2/CH_3CN (9:1) with $TBAPF_6$ (0.1 M) as the support electrolyte at a scan rate of 100 mV/s, except for the titrations with fluoride at 200 mV/s.

4.5. Electrochemical polymerization of 1

Cyclic voltammetry measurements were performed on a CH Instruments 660A Electrochemical Workstation with iR compensation, using anhydrous dichloromethane as the solvent. The electrodes were glassy carbon, platinum wire, and silver wire as the working, counter, and reference electrodes, respectively. All solutions were degassed (Ar) and contained monomer substrates in

concentrations ca. 2×10^{-4} M, together with $TBAPF_6$ (0.1 M) as the supporting electrolyte. All measurements are referenced against the $E_{1/2}$ of Fc/Fc^+ redox couple.

4.6. Materials

Unless otherwise stated, all reagents were purchased from Aldrich and used without additional purification. The solvents for spectroscopic studies were of spectroscopic grade and used as received. 5,6-Diamino-2-(4,5-bis(propylthio)-1,3-dithio-2-ylidene)benzo[*d*][1,3]dithiole[9] with 1,2-di(1*H*-2-pyrrolyl)-ethane-1,2-dione[10] were prepared following the literature procedures.

TTF-fused DPQ (***1***): A mixture of 5,6-diamino-2-(4,5-bis(propylthio)-1,3-dithio-2-ylidene)benzo[*d*][1,3]dithiole (180 mg, 0.4 mmol) and 1,2-di(1*H*-2-pyrrolyl)-ethane-1,2-dione (77.9 mg, 0.4 mmol) in glacial acetic acid (35 mL) was heated at 120 °C for 5 h under argon. The solvent was removed in vacuum and the crude product was purified by flash column chromatography on silica gel eluting with dichloromethane to give the *title compound* **1** (108 mg, 50%) as a dark-red solid. ^{1}H NMR (CD_2Cl_2, 300 MHz) δ: 9.65 (s, 2H), 7.72 (s, 2H), 7.03–7.00 (2×dd, J=1.5, 2.64 Hz, 2H), 6.92–6.90 (2×dd, J=1.32, 2.46 Hz, 2H), 6.26–6.25 (2×dd, J=2.64 Hz, 2H), 2.85–2.81 (t, J=7.2 Hz, 4H), 1.71–1.64 (m, 4H), 1.04–1.00 (t, J=7.2 Hz, 6H). ^{13}C NMR (CD_2Cl_2) δ: 142.6, 138.8, 137.9, 128.2, 127.1, 120.5, 118.5, 112.0, 109.1, 37.6, 22.4, 12.1. Selected IR data (KBr pellet, cm^{-1}): 3392, 3272, 2959, 2926, 2869, 1548, 1522, 1442, 1389, 1341, 1291, 1237, 1210, 1134, 1120, 1096, 1037, 933, 885, 854, 776, 752, 729, 590, 490. MS (EI) m/z: 584 (M^+, 100%). Anal. Calcd for $C_{26}H_{24}N_4S_6$: C, 53.39; H, 4.14; N 9.58. Found C, 53.72; H, 4.19; N, 9.25. Single crystals suitable for X-ray analysis were obtained by slow evaporation of a CH_2Cl_2 solution of **1**.

4.7. Crystallography

A dark orange rod-like crystal of **1** was mounted on a Stoe Mark II-Imaging Plate Diffractometer System (Stoe & Cie, 2002)[14] equipped with a graphite-monochromator. Data collection was performed at −100 °C using Mo Kα radiation (λ=0.71073 Å); 180 exposures (6 min per exposure) were obtained at an image plate distance of 135 mm, φ=0° with the crystal oscillating through 1° in ω. The resolution was D_{min}–D_{max} 0.82–24 Å. The structures were solved by direct methods using the program SHELXS-97[15] and refined by full matrix least-squares on F^2 with SHELXL-97.[16] The NH hydrogen atoms were derived from FOURIER difference maps and freely refined while the remaining hydrogen atoms were included in calculated positions and treated as riding atoms using SHELXL-97 default parameters. All non-hydrogen atoms were refined anisotropically. No absorption correction was applied. Crystal data has been deposited at the Cambridge Crystallographic Data Centre, CCDC 811625 (**1**). Copy of the data can be obtained, free of charge, on application to CCDC, 12 Union Road, Cambridge CB2 1EZ, UK [fax: +44 (0)1223 336033 or e-mail: deposit@ccdc.cam.ac.uk].

Acknowledgements

This work was supported by the Swiss National Science Foundation (grant no. 200020-130266/1).

Supplementary data

Supplementary data associated with this article can be found in the online version, at doi:10.1016/j.tet.2011.11.087. These data include MOL files and InChiKeys of the most important compounds described in this article.

References and notes

1. (a) Sessler, J. L.; Gale, P. A.; Cho, W. S. *Anion Receptor Chemistry*; Royal Society of Chemistry: Cambridge, UK, 2006; (b) Caltagirone, C.; Gale, P. A. *Chem. Soc. Rev.* **2009**, *38*, 520; (c) Sessler, J. L.; Seidel, D. *Angew. Chem., Int. Ed.* **2003**, *42*, 5134; (d) Suksai, C.; Tuntulani, T. *Chem. Soc. Rev.* **2003**, *32*, 192; (e) Gale, P. A.; Garcia-Garrido, S. E.; Garric, J. *Chem. Soc. Rev.* **2008**, *37*, 151; (f) Hudson, Z. M.; Wang, S. *Acc. Chem. Res.* **2009**, *42*, 1584.
2. (a) Martínez-Máñez, R.; Sancenón, F. *Chem. Rev.* **2003**, *103*, 4419; (b) Nishiyabu, R.; Anzenbacher, P., Jr. *J. Am. Chem. Soc.* **2005**, *127*, 8270; (c) Palacios, M. A.; Nishiyabu, R.; Marquez, M.; Anzenbacher, P., Jr. *J. Am. Chem. Soc.* **2007**, *129*, 7538.
3. (a) Lin, Z.; Zhao, Y.; Duan, C.; Zhang, B.; Bai, Z. *Dalton Trans.* **2006**, 3678; (b) Jiménez, D.; Martínez-Máñez, R.; Sancenón, F.; Ros-Lis, J. V.; Juan Soto, J.; Benito, Á.; García-Breijo, E. *Eur. J. Inorg. Chem.* **2005**, 2393; (c) Fillaut, J.-L.; Andriès, J.; Toupet, L.; Desvergne, J.-P. *Chem. Commun.* **2005**, 2924; (d) Mizuno, T.; Eller, L.; Wei, W.-H.; Sessler, J. L. *J. Am. Chem. Soc.* **2002**, *124*, 1134; (e) Anzenbacher, P., Jr.; Palacios, M. A.; Jursíková, K.; Marquez, M. *Org. Lett.* **2005**, *7*, 5027; (f) Ghosh, T.; Maiya, B. G.; Wong, M. W. *J. Phys. Chem. A* **2004**, *108*, 11249.
4. (a) Hudnall, T. W.; Chiu, C.-W.; Gabbai, F. P. *Acc. Chem. Res.* **2009**, *42*, 388; (b) Lee, C.-H.; Miyaji, H.; Yoon, D.-W.; Sessler, J. L. *Chem. Commun.* **2008**, 24.
5. (a) Anzenbacher, P., Jr.; Tyson, D. S.; Jursíková, K.; Castellano, F. N. *J. Am. Chem. Soc.* **2002**, *124*, 6232; (b) Pohl, R.; Aldakov, D.; Kubát, P.; Jursíková, K.; Marquez, M.; Anzenbacher, P., Jr. *Chem. Commun.* **2004**, 1282; (c) Sessler, J. L.; Pantos, G. D.; Katayev, E.; Lynch, V. M. *Org. Lett.* **2003**, *5*, 4141; (d) Ghosh, T.; Maiya, B. G.; Samanta, A. *Dalton Trans.* **2006**, 795; (e) Sessler, J. L.; Maeda, H.; Mizuno, T.; Lynch, V. M.; Furuta, H. *Chem. Commun.* **2002**, 862.
6. (a) *TTF Chemistry. Fundamentals and Applications of Tetrathiafulvalene*; Yamada, J., Sugimoto, T., Eds.; Springer: Berlin, 2004; (b) Canevet, D.; Sallé, M.; Zhang, G.; Zhang, D.; Zhu, D. *Chem. Commun.* **2009**, 2245; (c) Delahaye, S.; Loosli, C.; Liu, S.-X.; Decurtins, S.; Labat, G.; Neels, A.; Loosli, A.; Ward, T. R.; Hauser, A. *Adv. Funct. Mater.* **2006**, *16*, 286; (d) Frère, P.; Skabara, P. J. *Chem. Soc. Rev.* **2005**, *34*, 69.
7. (a) Lu, H.; Xu, W.; Zhang, D.; Chen, C.; Zhu, D. *Org. Lett.* **2005**, *7*, 4629; (b) Lu, H.; Xu, W.; Zhang, D.; Zhu, D. *Chem. Commun.* **2005**, 4777; (c) Nielsen, K. A.; Jeppesen, J. O.; Levillain, E.; Becher, J. *Angew. Chem., Int. Ed.* **2003**, *42*, 187; (d) Nielsen, K. A.; Cho, W. S.; Lyskawa, J.; Levillain, E.; Lynch, V. M.; Sessler, J. L.; Jeppesen, J. O. *J. Am. Chem. Soc.* **2006**, *128*, 2444; (e) Benhaoua, C.; Mazari, M.; Mercier, N.; Le Derf, F.; Sallé, M. *New J. Chem.* **2008**, *32*, 913; (f) Zhao, B.-T.; Blesa, M. J.; Le Derf, F.; Canevet, D.; Benhaoua, C.; Mazari, M.; Allain, M.; Sallé, M. *Tetrahedron* **2007**, *63*, 10768; (g) Nielsen, K. A.; Cho, W. S.; Jeppesen, J. O.; Lynch, V. M.; Becher, J.; Sessler, J. L. *J. Am. Chem. Soc.* **2004**, *126*, 16296; (h) Nielsen, K. A.; Cho, W. S.; Sarova, G. H.; Petersen, B. M.; Bond, A. D.; Becher, J.; Jensen, F.; Guldi, D. M.; Sessler, J. L.; Jeppesen, J. O. *Angew. Chem., Int. Ed.* **2006**, *45*, 6848.
8. Bejger, C.; Park, J. S.; Silver, E. S.; Sessler, J. L. *Chem. Commun.* **2010**, 7745.
9. Jia, C.-Y.; Liu, S.-X.; Tanner, C.; Leiggener, C.; Neels, A.; Sanguinet, L.; Levillain, E.; Leutwyler, S.; Hauser, A.; Decurtins, S. *Chem.—Eur. J.* **2007**, *13*, 3804.
10. Black, C. B.; Andrioletti, B.; Try, A. C.; Ruiperez, C.; Sessler, J. L. *J. Am. Chem. Soc.* **1999**, *121*, 10439.
11. (a) Devic, T.; Avarvari, N.; Batail, P. *Chem.—Eur. J.* **2004**, *10*, 3697; (b) Wu, J.-C.; Liu, S.-X.; Neels, A.; Le Derf, F.; Sallé, M.; Decurtins, S. *Tetrahedron* **2007**, *63*, 11282; (c) Jia, C.; Liu, S.-X.; Ambrus, C.; Neels, A.; Labat, G.; Decurtins, S. *Inorg. Chem.* **2006**, *45*, 3152; (d) Wu, J. C.; Liu, S.-X.; Keene, T. D.; Neels, A.; Mereacre, V.; Powell, A. K.; Decurtins, S. *Inorg. Chem.* **2008**, *47*, 3452; (e) Goze, C.; Dupont, N.; Beitler, E.; Leiggener, C.; Jia, H.-P.; Monbaron, P.; Liu, S.-X.; Neels, A.; Hauser, A.; Decurtins, S. *Inorg. Chem.* **2008**, *47*, 11010; (f) Wu, J.-C.; Dupont, N.; Liu, S.-X.; Neels, A.; Hauser, A.; Decurtins, S. *Chem. Asian J.* **2009**, *4*, 392; (g) Liu, S.-X.; Dolder, S.; Rusanov, E. B.; Stoeckli-Evans, H.; Decurtins, S. *C.R. Chim.* **2003**, *6*, 657; (h) Jaggi, M.; Blum, C.; Dupont, N.; Grilj, J.; Liu, S.-X.; Hauser, J.; Hauser, A.; Decurtins, S. *Org. Lett.* **2009**, *11*, 3096.
12. Sessler, J. L.; Cho, D. G.; Lynch, V. *J. Am. Chem. Soc.* **2006**, *128*, 16518.
13. Wang, T.; Yan, X.-P. *Chem.—Eur. J.* **2010**, *16*, 4639.
14. Stoe & Cie. *IPDS Software*; Stoe & Cie: Darmstadt, Germany, 2005.
15. Sheldrick, G. M. *Acta Crystallogr.* **1990**, *A46*, 467.
16. Spek, A. L. *J. Appl. Crystallogr.* **2003**, *36*, 7.